South African Journal of Chemical Engineering 30 (2019) 28–41

Contents lists available at ScienceDirect

South African Journal of Chemical Engineering

journal homepage: www.elsevier.com/locate/sajce

# Synergistic combination effect of clove essential oil extract with basil and atlas cedar oil on the corrosion inhibition of low carbon steel

Roland Tolulope Loto*, Tiwa Olukeye, Eugene Okorie

*Department of Mechanical Engineering, Covenant University, Ota, Ogun State, Nigeria*

ARTICLE INFO

*Keywords:*
Carbon steel
Corrosion
Oil
Inhibitor

ABSTRACT

Clove essential oil extracts was separately admixed with basil oil extract (CLB) and atlas cedar oil extract (CLA), and studied for their corrosion inhibition properties on low carbon steel in 0.5 M $H_2SO_4$ and HCl solutions by coupon analysis, potentiodynamic polarization, open circuit potential measurement and optical microscopy. Results showed the two admixed inhibitor compounds performed effectively at most concentrations with optimal inhibition efficiencies of 95.48% and 95.32% in $H_2SO_4$ solution while in HCl the corresponding values are 92.7% and 97.98%. CLB and CLA showed mixed inhibiting properties though shift in corrosion potential and Tafel slope values indicates dominant cathodic inhibition and higher cathodic exchange current density. Severe general deterioration was visible on the morphology of control (no inhibitor) steels in $H_2SO_4$ while the morphology of the control steel from HCl showed extensive localized deterioration. Addition of CLB and CLA significantly improved the morphology of the steel in both acid solutions signifying effective corrosion inhibition. The open circuit potential plots of the carbon steel in both acids showed significant potential transients due to thermodynamic instability in the presence of the inhibitors. However, the corrosion potential plots were significantly electropositive relative to the plot of the control specimen with final values −0.448V and −0.452V in $H_2SO_4$, and -0.476V in HCl (CLA).

## 1. Introduction

The global steel industry is the critical backbone of the industrialized value chain. Carbon steel has been an essential base material for significant economic sectors and has extensive applications in large tonnages as material of construction for structures and equipment (Ocheri et al., 2017; Winnik, 2008). These steels are readily available with relatively low cost compared to stainless steels, can easily fabricated and are recyclable. Low-carbon steels are particularly important due to their excellent welding and forming abilities. However, they are vulnerable to corrosion due to the porosity of the oxide that forms on their surface when exposed to corrosive agents. The porous oxide serves as sites where crevices etc. traps moisture and $H_2O$, creating operational problems of equipment and plants, accelerating corrosion attack and reduced lifespan (Zarras and Stenger-Smith, 2014; Ahmad, 2006; Gardner, 2008). The extensive application of low carbon steels coupled with its weak corrosion resistance results in very high corrosion cost. The costs is due to repair of damaged equipment and structures, industrial downtime and process disruptions, environmental pollution due to leakages etc. One of the most effective methods of alleviating the corrosion vulnerability of carbon steels is to alter the environment of application of these steels through the addition of limited quantities of chemical compounds known as corrosion inhibitors (Saranya et al., 2016). Development or formulation of green chemical compounds for corrosion inhibition is an important step in the research for alternatives to the dominant, inorganic/organic and toxic chemical compounds for corrosion inhibition (Roy et al., 2014). Most corrosion inhibitors generally act through adsorption, creating an impenetrable film on the steel surface (Verma et al., 2016, 2017). In many cases the corrosive anions attacks the steel surface resulting in negatively charge surface causing the attraction of protonated inhibitor cations onto the steel surface (Thomas and Kim, 2013). Application of essential oil extracts for corrosion inhibition have been very promising, however their inhibition performance is heavily concentration dependent which can be dangerous when there are fluctuations in the physical state and properties of the corrosive environment (Narayanasamy et al., 2009; Afia et al., 2014; Rekkab et al., 2012; Dahmani et al., 2012;. Hamdani et al., 2015; El ouadi et al., 2014; Hmamou et al., 2013; Bouoidina et al., 2017; Loto et al., 2011; Loto and Oghenerukewe, 2016; Loto, 2016; Loto, 2018a,b; Loto, 2018a,b). Synergistic combination effect of essential oil extracts have been proven to be effective at all concentrations studied (Loto et al, 2018, 2019; Loto and Olowoyo, 2018). In contribution to the

* Corresponding author.
*E-mail address:* tolu.loto@gmail.com (R.T. Loto).

https://doi.org/10.1016/j.sajce.2019.08.001
Received 2 May 2019; Received in revised form 20 August 2019; Accepted 23 August 2019

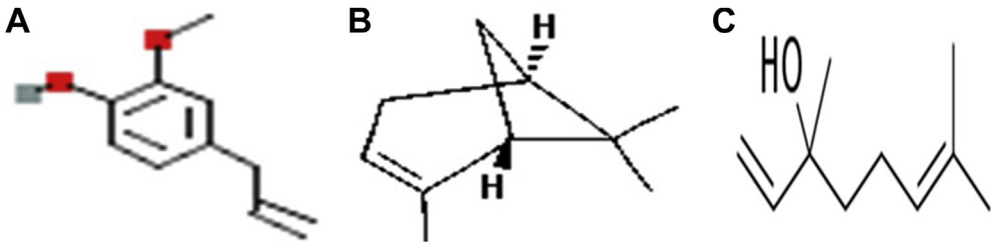


**Fig. 1.** Major component of (a) clove oil (eugenol), (b) atlas cedar oil (alpha-pinene) and (c) basil oil (linalool).

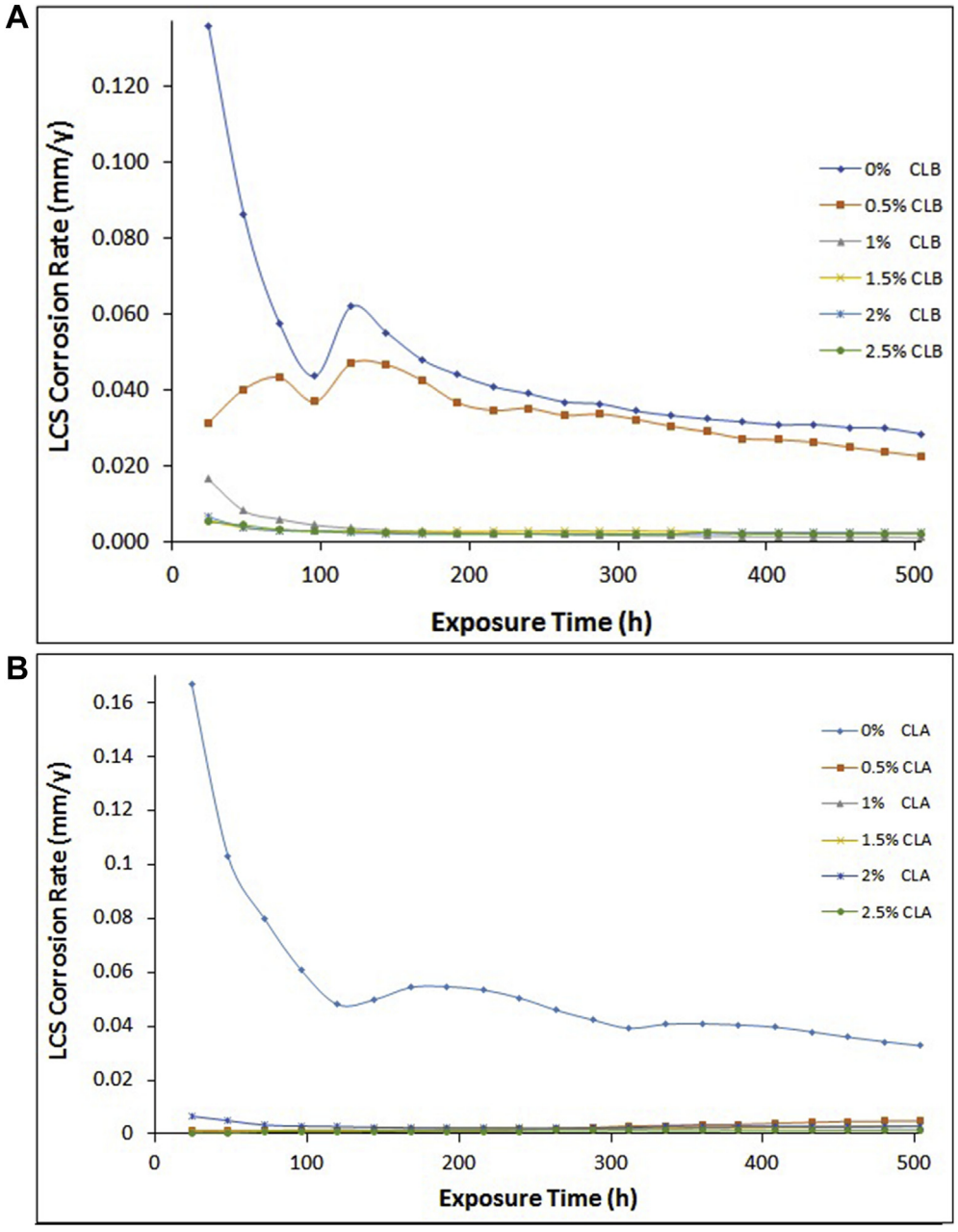


**Fig. 2.** Plot of LCS corrosion rate versus exposure time at specific inhibitor concentrations in $H_2SO_4$ solution (a) CLB inhibitor and (b) CLA inhibitor.

research on naturally occurring compounds for effective corrosion inhibition and their synergistic combination effect for improved performance, this research focuses on the synergistic combination effect of clove oil with basil oil, and clove oil with altas cedar oil. The individual performance of these oils are well above average in some cases but can be improved further (El-Hajjaji et al., 2017; Adardour et al., 2018; Prajapati and Vashi, 2017; Halambek et al., 2013; Loto and Loto, 2019; Idouhli et al., 2017).

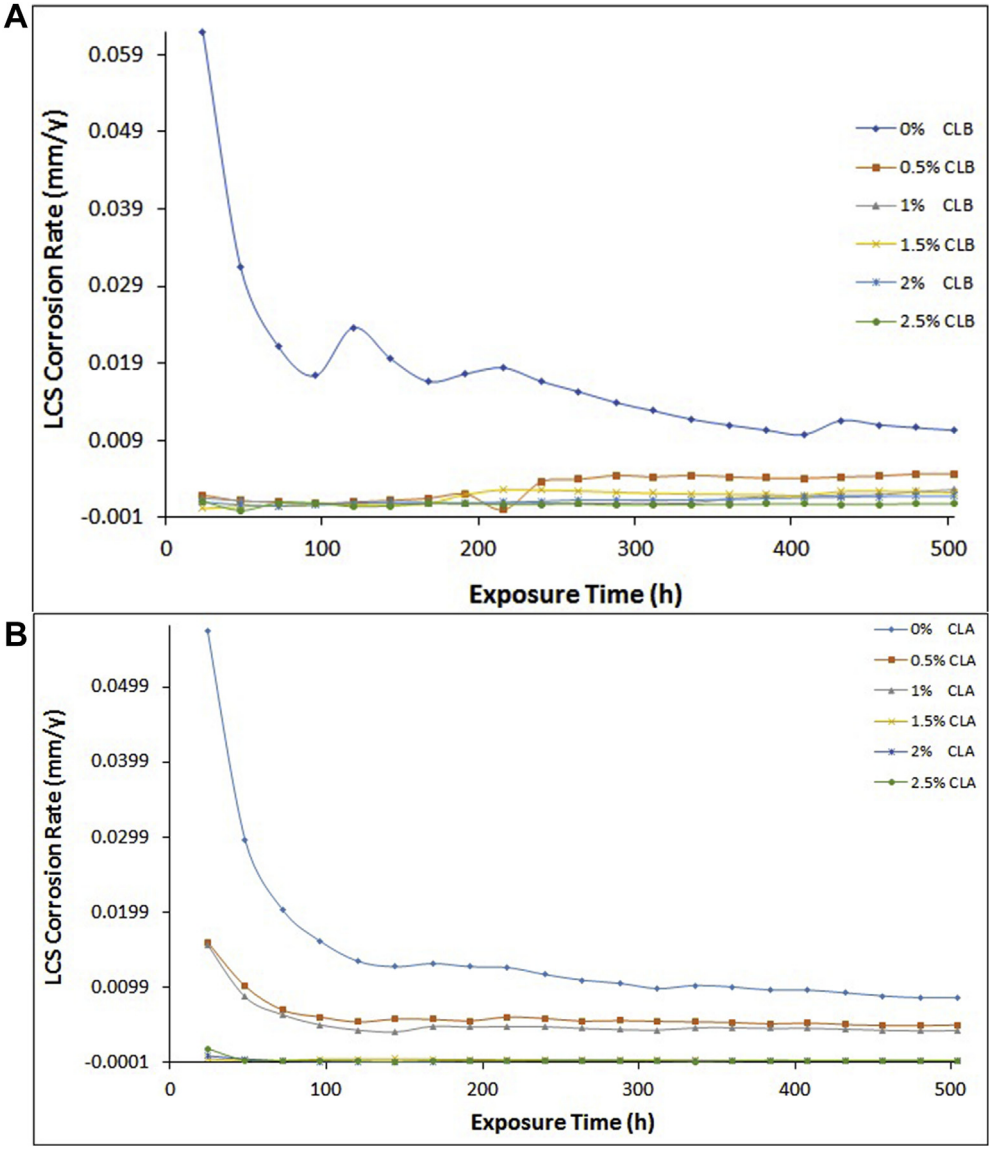


**Fig. 3.** Plot of LCS corrosion rate versus exposure time at specific inhibitor concentrations in HCl solution (a) CLB inhibitor and (b) CLA inhibitor.

## 2. Experimental methods

### 2.1. Materials and preparation

Low carbon steel (LCS) with circular dimension (thickness, 6 mm and diameter, 12 mm), purchased from the open market has nominal weight composition (wt. %) of 0.8% Mn, 0.04% P, 0.05% S, 0.16% C and 98.95% Fe. The steel was cut into 28 individual specimens, grinded with emery papers (80–2500 grits), polished with 6 µm diamond paste and thereafter washed with distilled water and propanone. Clove, atlas cedar and basil oil extracts were purchased from NOW Foods, USA. Fig. 1(a) – (c) shows the major component the oil extracts. Synergistic inhibition properties of the oil extracts was studied through admixture of clove oil with basil oil (CLB), and clove oil with atlas cedar oil (CLA) in ratio 1:1. Their combined admixtures (CLB) and (CLA) were formulated in volumetric concentrations of 0.5%, 1%, 1.5%, 2% and 2.5% per 200 mL of 0.5 M $H_2SO_4$ and HCl solution.

### 2.2. Coupon measurement

LCS specimens were separately immersed 200 mL of 0.5 M H2SO4 and HCl solutions for 504 h and weighed at every 24 h. Corrosion rate, $C_R$ (mm/y) was determined as follows;

$$C_R = \left[\frac{87.6\omega}{DAt}\right] \quad (1)$$

$\omega$ is the weight loss (g), $D$ is the density (g/cm$^3$), $A$ is the total exposed surface area of LCS specimen (cm$^2$), 87.6 is a constant and $t$ is the time (h). Inhibition efficiency ($\eta$) was determined as follows;

$$\eta = \left[\frac{\omega_1 - \omega_2}{\omega_1}\right] \times 100 \quad (2)$$

$\omega_1$ and $\omega_2$ are the weight loss of LCS at specific CLB and CLA concentrations. Surface coverage was determined from equation 6:

$$\theta = \left[1 - \frac{\omega_2}{\omega_1}\right] \quad (3)$$

where $\theta$ is the degree of inhibitor coverage on LCS.

### 2.3. Potentiodynamic polarization

Analysis of the corrosion polarization of LCS was done at 30 °C ambient temperature. A ternary electrode configuration (Pt rod counter

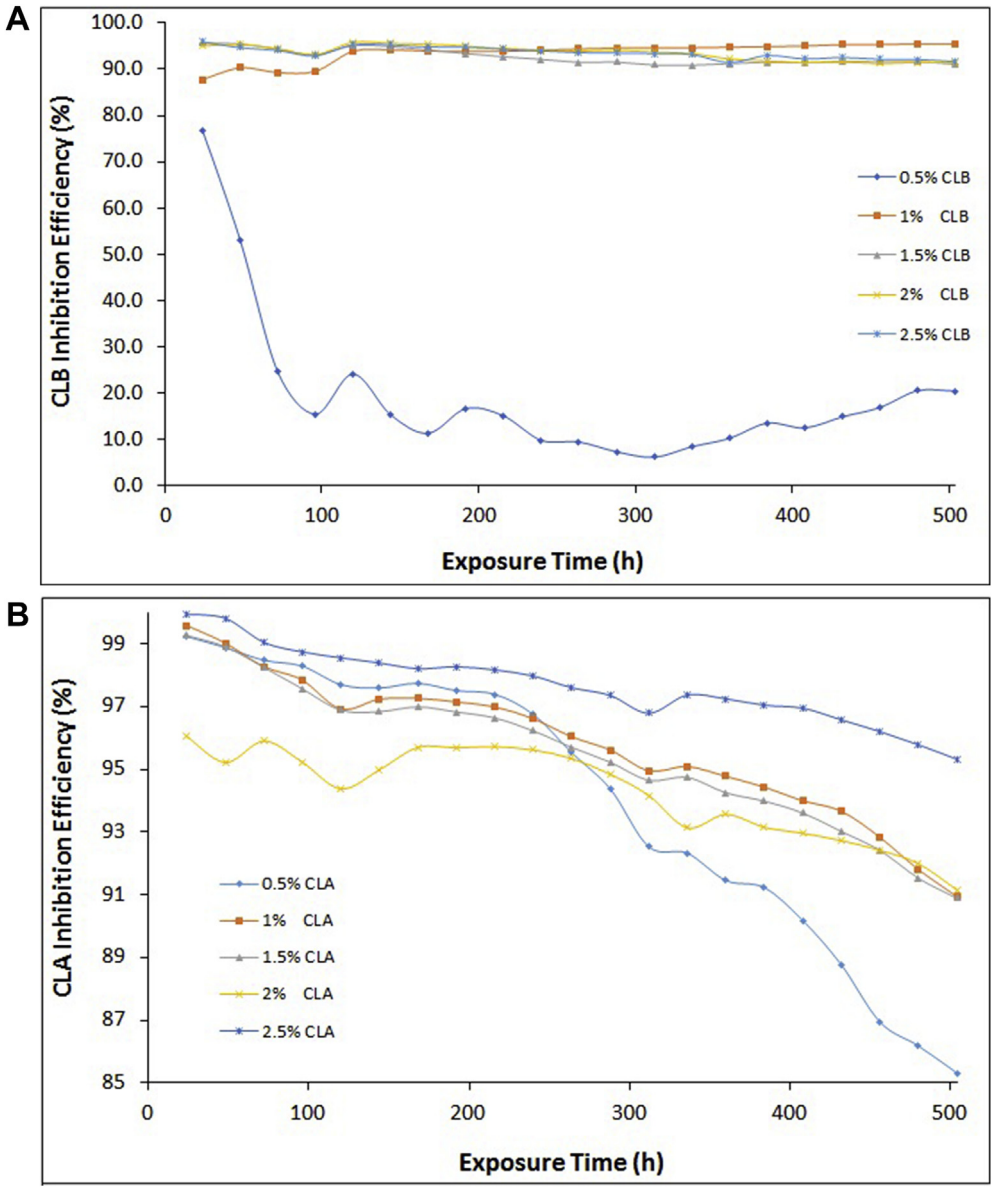


**Fig. 4.** Plot of inhibition efficiency versus exposure time from $H_2SO_4$ solution (a) CLB inhibitor and (b) CLA inhibitor.

electrode, Ag/AgCl reference electrode with 3 M KCl electrolyte at a pH of 6.5 and cylindrical LCS working electrodes) within a glass cell containing 200 mL of acid ($H_2SO_4$, HCl)-inhibitor (CLB, CLA) solution and linked to Digi-Ivy 2311 potentiostat. The LCSW working electrode was embedded in acylic mounts with limited surface area of 1.13 $cm^2$. Polarization plots were obtained at scan rates of 0.0015 V/s at potentials of −0.75 V to +1.5 V. Corrosion current density $J_{cr}$ (A/$cm^2$) and corrosion potential $E_{cr}$ (V) values were obtained Tafel extrapolation. Corrosion current $I_{cr}$ (A) was obtained from anodic-cathodic polarization plot intercept. Corrosion rate, $C_R$ (mm/y) was calculated as follows;

$$C_R = \frac{0.00327 \times J_{cr} \times E_v}{D} \tag{4}$$

$E_v$ is the equivalent weight (g) of LCS, 0.00327 is a constant, and $D$ is the density (g/$cm^3$). Inhibition efficiency $\eta$ (%) was determined from equation;

$$\eta_2 = \left[1 - \left(\frac{C_{R2}}{C_{R1}}\right)\right] \times 100 \tag{5}$$

$C_{R2}/C_{R1}$ is the ration of corrosion rate of LCS with and without the admixed oil extracts in the acid solution.

### 2.4. Optical microscopy studies

Optical micrographs of corroded LCS morphology from control acid solutions was analysed and compared to CLB and CLA inhibited LCS morphology after corrosion test with Omax trinocular metallurgical microscope using ToupCam software.

## 3. Result and discussion

### 3.1. Coupon measurement

The plots of LCS corrosion rates, CLB inhibition efficiencies and CLA inhibition efficiencies versus exposure time from coupon measurement is shown from Fig. 2(a) to Fig. 5(b). Figs. 2(a) and 3(b) shows the plot of LCS corrosion rates versus exposure time in $H_2SO_4$ and HCl solution in the presence of CLB and CLA inhibitor compound while Figs. 4(a) and 5(b) shows the plots of CLB and CLA inhibition efficiencies versus

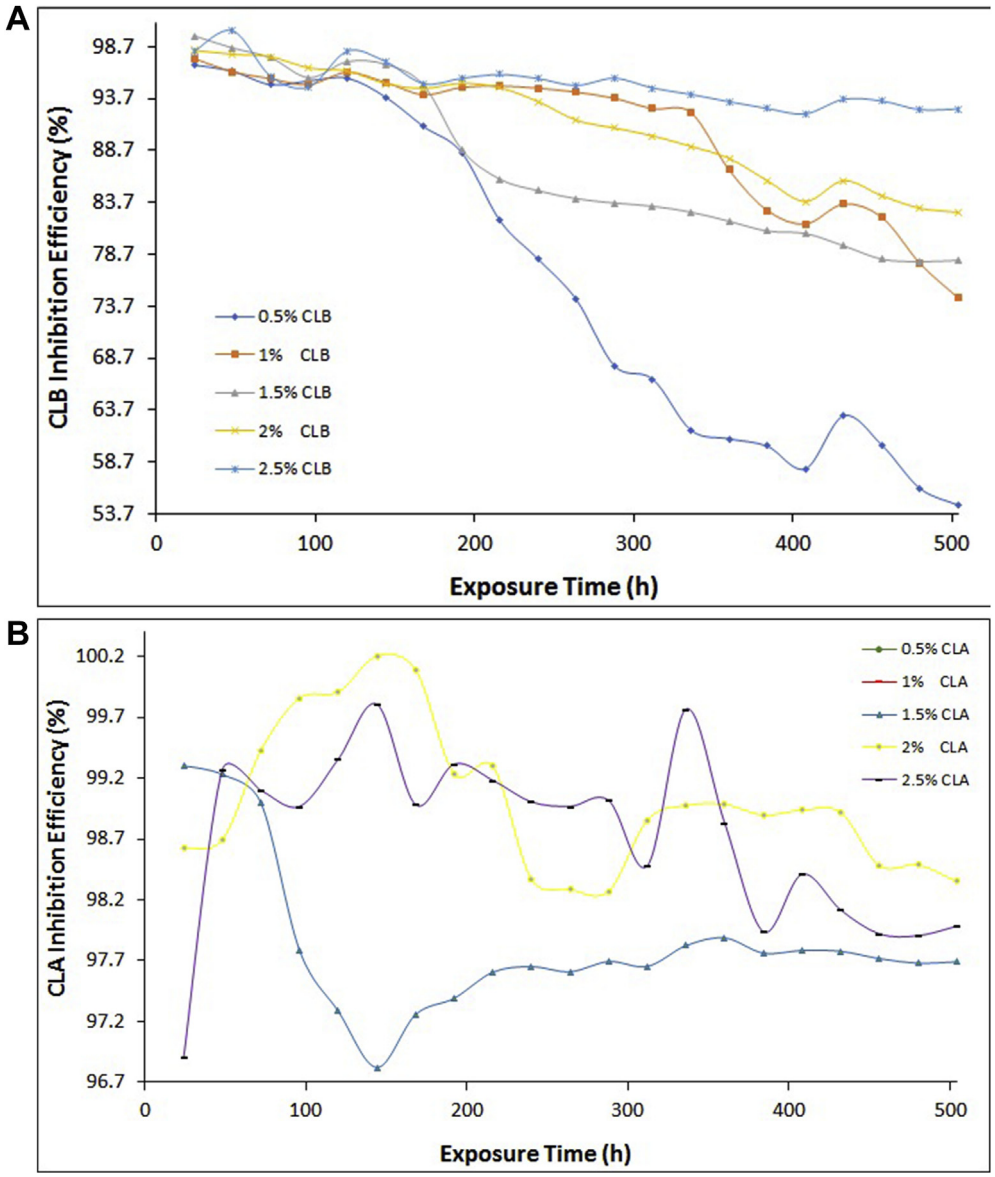


**Fig. 5.** Plots of inhibition efficiency versus exposure time from HCl solution (a) CLB inhibitor and (b) CLA inhibitor.

**Table 1**
Results of LCS corrosion inhibition in $H_2SO_4$ solution at 0%–2.5% CLB and CLA concentrations from coupon analysis at 504 h (n = 1).

| CLB Inhibitor | | | | | CLA Inhibitor | | | | |
|---|---|---|---|---|---|---|---|---|---|
| Samples | CLB Conc. (%) | CLB Weight Loss (g) | LCS Corrosion Rate (mm/y) | CLB Inhibition Efficiency (%) | Samples | CLA Conc. (%) | CLA Weight Loss (g) | LCS Corrosion Rate (mm/y) | CLA Inhibition Efficiency (%) |
| A | 0 | 7.794 | 0.029 | – | A | 0 | 8.909 | 0.033 | – |
| B | 0.5 | 6.198 | 0.023 | 20.48 | B | 0.5 | 1.308 | 0.005 | 85.32 |
| C | 1 | 0.352 | 0.001 | 95.48 | C | 1 | 0.807 | 0.003 | 90.94 |
| D | 1.5 | 0.693 | 0.003 | 91.11 | D | 1.5 | 0.812 | 0.003 | 90.89 |
| E | 2 | 0.677 | 0.002 | 91.32 | E | 2 | 0.788 | 0.003 | 91.16 |
| F | 2.5 | 0.650 | 0.002 | 91.66 | F | 2.5 | 0.417 | 0.002 | 95.32 |

exposure time in $H_2SO_4$ and HCl solutions. Tables 1 and 2 depict the final LCS weight loss and corrosion rate, and CLB and CLA inhibition efficiency in $H_2SO_4$ and HCl solution at 504 h. The corrosion rate values of LCS at 0% CLB and CLA concentration [Figs. 2(a, b) and 3(a, b)] in both acid solutions significantly contrast the values obtained at higher CLB and CLA concentrations. The observation is due to the oxidation of LCS in the presence of $SO_4^{2-}$ and $Cl^-$ anions. This results in the release of $Fe^{2+}$ cations and $H_2$ gas in the acid solutions. The corrosion rate values of LCS in $H_2SO_4$ solution where generally higher than the values obtained in HCl due to the higher ionization potenial of $H_2SO_4$ in $H_2O$ and the tendency of $SO_4^{2-}$ to degrade the entire surface o LCS compare to $Cl^-$ whose electrochemical action on LCS tends to be localized over the entire steel surface. Addition of CLB and CLA oil extracts (corrosion inhibitor) to the acid media significantly changed the dynamics of the redox electrochemical processes resulting in visible reduction in LCS corrosion rate values. The corrosion inhibition performance of CLB and

**Table 2**
Results of LCS corrosion inhibition in HCl solution at 0%–2.5% CLB and CLA concentrations from coupon analysis at 504 h (n = 1).

| CLB Inhibitor | | | | | CLA Inhibitor | | | | |
|---|---|---|---|---|---|---|---|---|---|
| Samples | CLB Conc. (%) | CLB Weight Loss (g) | LCS Corrosion Rate (mm/y) | CLB Inhibition Efficiency (%) | Samples | CLA Conc. (%) | CLA Weight Loss (g) | LCS Corrosion Rate (mm/y) | CLA Inhibition Efficiency (%) |
| A | 0 | 2.807 | 0.010 | – | A | 0 | 2.330 | 0.009 | – |
| B | 0.5 | 1.276 | 0.005 | 54.54 | B | 0.5 | 1.342 | 0.005 | 42.40 |
| C | 1 | 0.716 | 0.003 | 74.47 | C | 1 | 1.136 | 0.004 | 51.26 |
| D | 1.5 | 0.614 | 0.002 | 78.12 | D | 1.5 | 0.054 | 0.0002 | 97.69 |
| E | 2 | 0.484 | 0.002 | 82.74 | E | 2 | 0.038 | 0.0001 | 98.35 |
| F | 2.5 | 0.205 | 0.001 | 92.70 | F | 2.5 | 0.047 | 0.0002 | 97.98 |

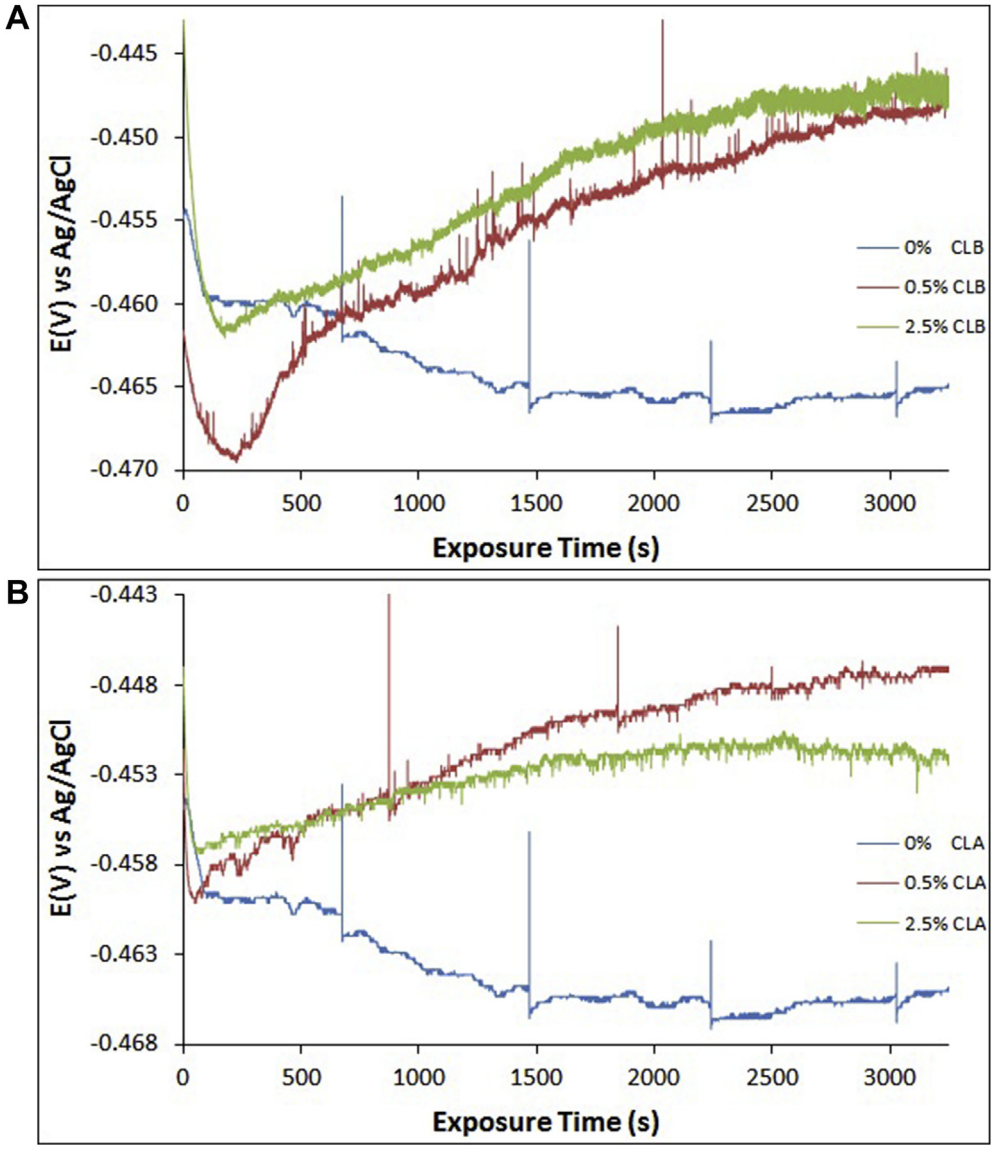


**Fig. 6.** OCP plots of LCS in 0.5 M $H_2SO_4$ at 0%, 0.5% and 2.5% CLB and CLA concentration (a) CLB inhibitor, and (b) CLA inhibitor.

CLA tends to be independent of concentration in $H_2SO_4$ solution compared to HCl media where slight dependence on concentration was observed. However, Fig. 2(a) shows CLB at 0.5% concentration performed pooly compared to CLA [Fig. 2(b)] which performed effectively at all concentrations. Fig. 3(a) shows increase in corrosion rate for CLB (0.5% concentration) beginning at 240 h while CLA in Fig. 3(b) shows poor performance at 0.5% and 1% concentration. The inhibition efficiency values of CLB and CLA [Figs. 4(a) and 5(b)] provides further insight on their corrosion inhibition performance. Fig. 4(a) shows relative stability of CLB (in $H_2SO_4$ solution) at 1%–2.5% CLB concentration with values generally above 90%, signifying effective corrosion inhibition. At 0.5% CLB, the corrosion rate value decreased from 76.87% at 24 h to values below 30% between 72h and 504 h. The corresponding performance of CLA in $H_2SO_4$ [Fig. 4(b)] was less satifactory as visible decrease in inhibition eficiency values was observed throughout the xposure hours, though at 504 h the values were generally above 90% (excluding CLA at 0.5% with inhibition efficiency of 85%), the observed decrease with respect to time shows the inhibition

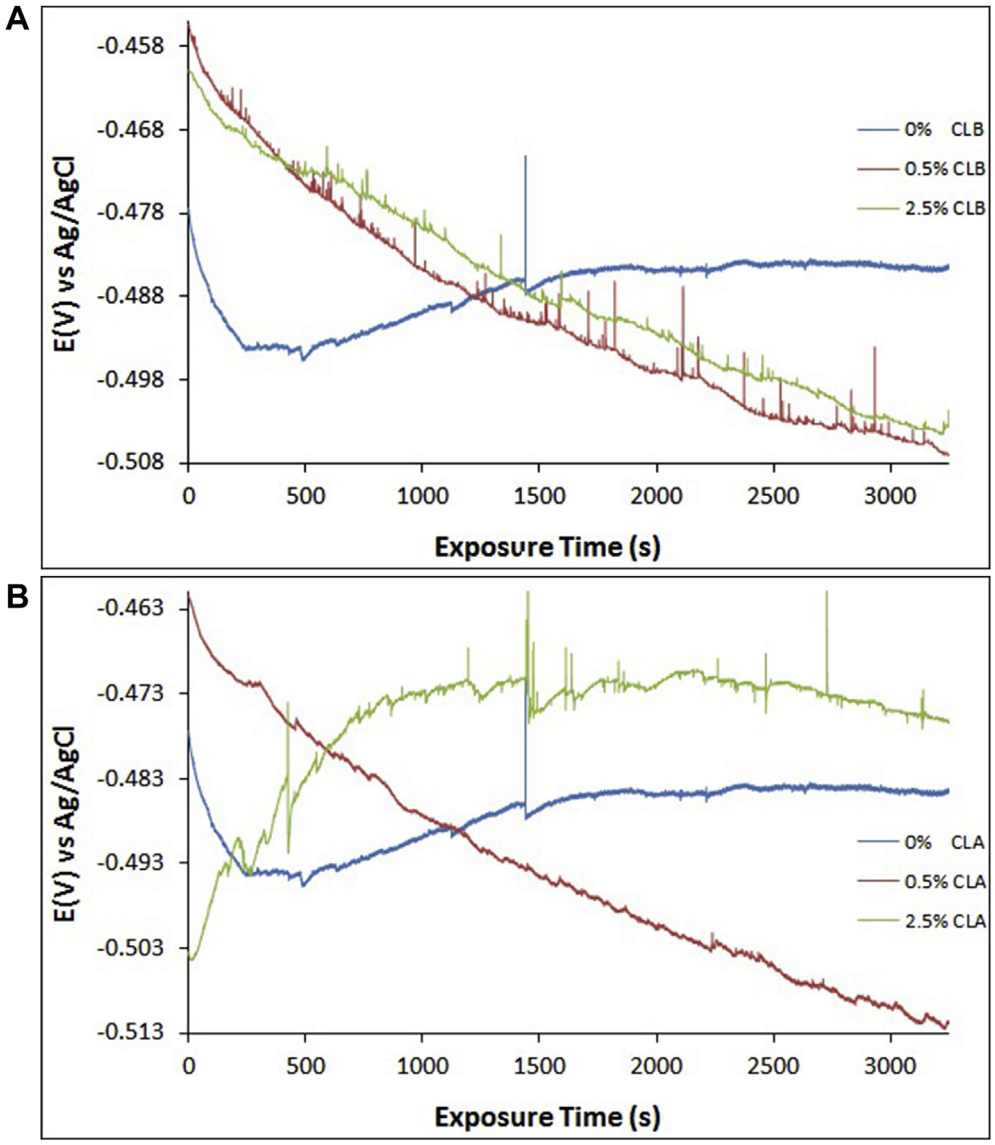


**Fig. 7.** OCP plots of LCS in 0.5 M HCl at 0%, 0.5% and 2.5% CLB and CLA concentration (a) CLB inhibitor, and (b) CLA inhibitor.

efficiency will continue to decrease. Similar observation occurred in Fig. 5(a) where the inhibition performance of CLB decreased with time from 0.5% to 2% CLB concentration. At 2.5% CLB, the inhibition efficiency value was relatively stable. CLA extract from 1.5% to 2.5% CLA concentration performed very effectively in HCl solution [Fig. 5(b)] with inhibition efficiency values varying between 96.8% and 100% during exposure. There was no decrease in value till 504 h. However, CLA performance at 0.5% and 1% CLA was less satisfactory; Fig. 5(b) shows the plots at the aformntioned concentrations initiated with inhibition efficiency of 72.79% at 24h and closed with values of 42.4% (0.5% CLA) and 51.26% (1% CLA). Comparison of the final inhibition efficiency values in Table 1 shows CLB and CLA inhibitor performed excellently with optimal inhibition values of 95.48% and 95.32% at 1% CLB and 2.5% CLA in $H_2SO_4$ solution while in HCl solution (Table 2) the optimal values are 92.7% at 2.5% CLB and 98.35% at 2% CLA.

### 3.2. Open circuit potential measurement (OCP)

Variation of LCS corrosion potential with exposure time at 0%, 0.5% and 2.5% CLB and CLA concentration from $H_2SO4$ solution is shown in Fig. 6(a) and (b) while Fig. 7(a) and (b) shows the LCS corrosion potential with exposure time from HCl solution. The OCP plot of LCS at 0% CLB and CLA concentration [Fig. 6(a) and (b) significantly shifted to electronegative potentials. The plot initiated at −0.455V (0s) and displaced sharply −0.459V at 82.35s after which the plot was thermodynamically stable to −0.460V at 608.70s. The plot progressively decreased to −0.465V at 1407.11s and thereafter was thermodynamically stable to 3250 s. The displacement to electronegative potentials is as a result gradual oxidation of the steel surface leading to the formation of oxides and breakdown of its surface properties of the steel. CLB and CLA inhibitor caused significant shift in corrosion potential to electropositive values due to their inhibition and corrosion protective properties on LCS. The progressive shift to these values shows CLB and CLA inhibitor gradually adsorbs on LCS surface shielding it from the debilitating effect of $SO_4^{2-}$ and $Cl^-$ anions responsible for corrosion in the acid solution. Nevertheless, the visible potential transients show competitive adsorption between the inhibitor molecules and corrosive anions. The OCP plots of LCS from HCl solution contrasts its behaviour in $H_2SO_4$. At 0.5% and 2.5% CLB [Fig. 7(a)], the corrosion potential shifted to more electronegative values than the plot at 0% CLB. This phenomenon is associated with high tendency of the steel to corrode and agrees with the poor inhibition performance of CLB at 0.5% CLB. However, comparing the plot at 2.5% CLB to the data obtained from weight loss, the displacement of the plot to electronegative values

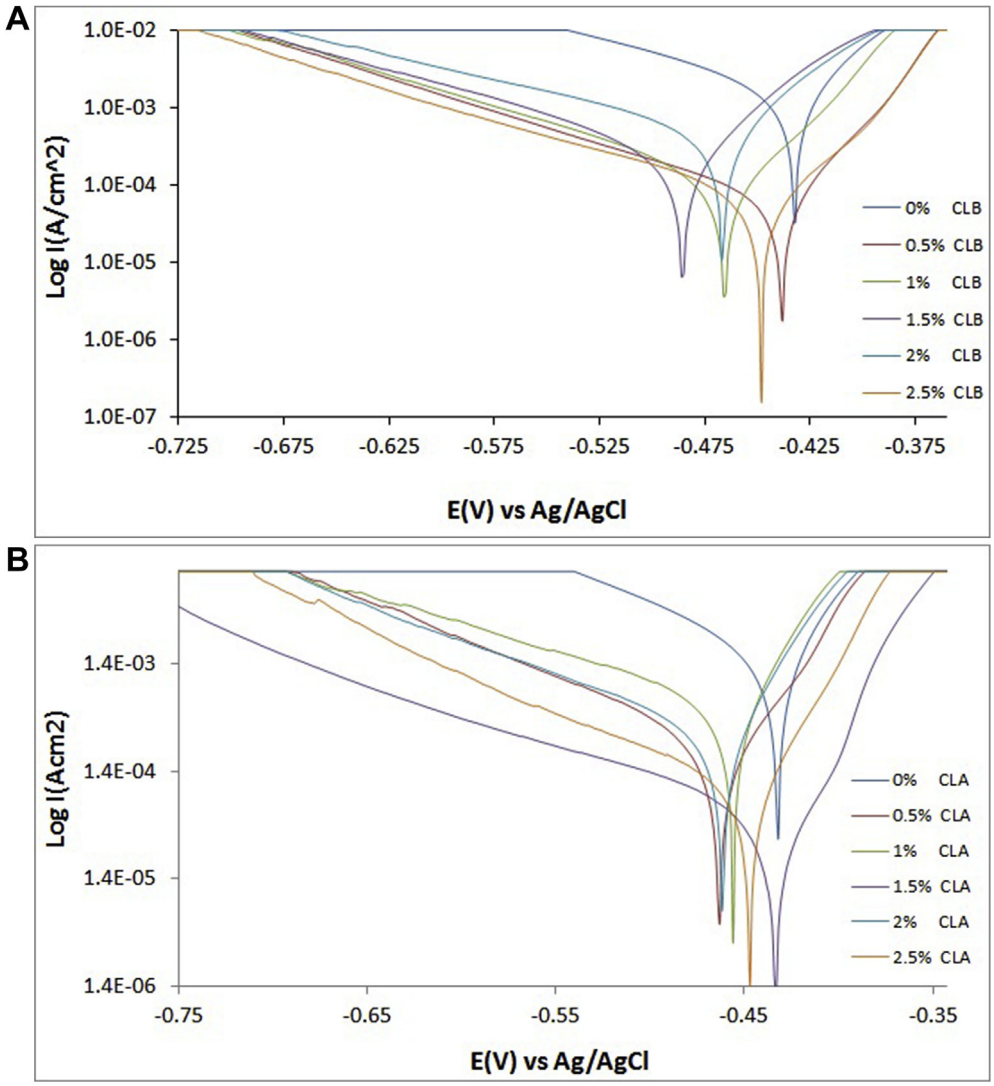


**Fig. 8.** Potentiodynamic polarization plots for LCS corrosion in HCl solution at 0%–2.5% inhibitor concentration (a) CLB inhibitor and (b) CLA inhibitor.

shows the presence CLB influences the active passive transition behaviour of the steel making it thermodynamically unstable and increasing its tendency to corrosion in the presence of $Cl^-$ anions. Comparing these observations to the plots in Fig. 7(b), the plots at 0.5% CLA was significantly electronegative relative to the plot at 0% CLA while the plot at 2.5% CLA was electropositive. This observation agrees with the results obtained from coupon measurement. At 0.5% CLA, CLA inhibitor performed poorly through the exposure hours; the plot at 0.5% CLA shows high tendency to corrode, displacing to −0.512V at 3250s. The plot at 2.5% CLA peaked at −0.476V at 3250s relative to the value obtained at 0% CLA (−0.484V). The potential transients at 2.5% CLA shows competitive absorption between the corrosive and inhibitor species is prevalent and there is strong possibility the protective film offered by CLA is effective but unstable.

### 3.3. Potentiodynamic polarization studies

Potentiodynamic polarization plots of LCS corrosion in 0.5M $H_2SO_4$ solution at 0%–2.5% CLB and CLA concentration are shown from Fig. 8(a) and 8(b), while and (b) shows the corresponding plots in HCl solution. Tables 3 and 4 shows the data obtained from the polarization plots. Similar to the observation from coupon analysis, the corrosion rates of the control LCS (0% CLB and CLA inhibitor) significantly differs from the inhibited steel due to the electrochemical action of the inhibitor molecules. At 0.5% inhibitor concentration CLA (59.61%) slightly outperforms CLB at 32.52% inhibition efficiency in $H_2SO_4$ solution which corresponds to corrosion rate values of 6.20 mm/y and 3.71 mm/y. Increase in inhibitor concentration from 1% to 2.5% significantly improved the inhibition efficiency of CLB and CLA inhibitor to values above 80% with peak value of 87.16% (2.5% CLB) and 92.1% (1.5% CLA). The inhibitor values show non-dependence on inhibitor concentration after 0.5%. Observation of the variation of LCS corrosion potential with respect to CLB and CLA concentration after 0% concentration shows higher tendency for cathodic inhibition. However, shift in potential shows CLB and CLA compound has mixed inhibition properties. The anodic Tafel slope values after 0% CLB and CLA is due to inhibition of anodic dissolution of the steel resulting in higher anodic exchange current density. Changes in the Tafel values after 0% inhibitor concentration also shows surface coverage of LCS surface by both inhibitors suppressed the electrochemical action of $SO_4^{2-}$ thus hindering them from oxidizing the steel surface. The extent of LCS corrosion damage in HCl solution (0% inhibitor concentration) was slightly lower at corrosion rate of 5.94 mm/y. Addition of CLB inhibitor to HCl solution from 0.5% to 2.5% CLB concentration results in inhibition efficiency value generally above 80%. Effective inhibition of LCS by CLA occurred after 0.5% CLA concentration. Observing the anodic and Tafel values from HCl solution, no visible change after 0% CLB and CLA concentration occurred, and increase in inhibitor concentration also did

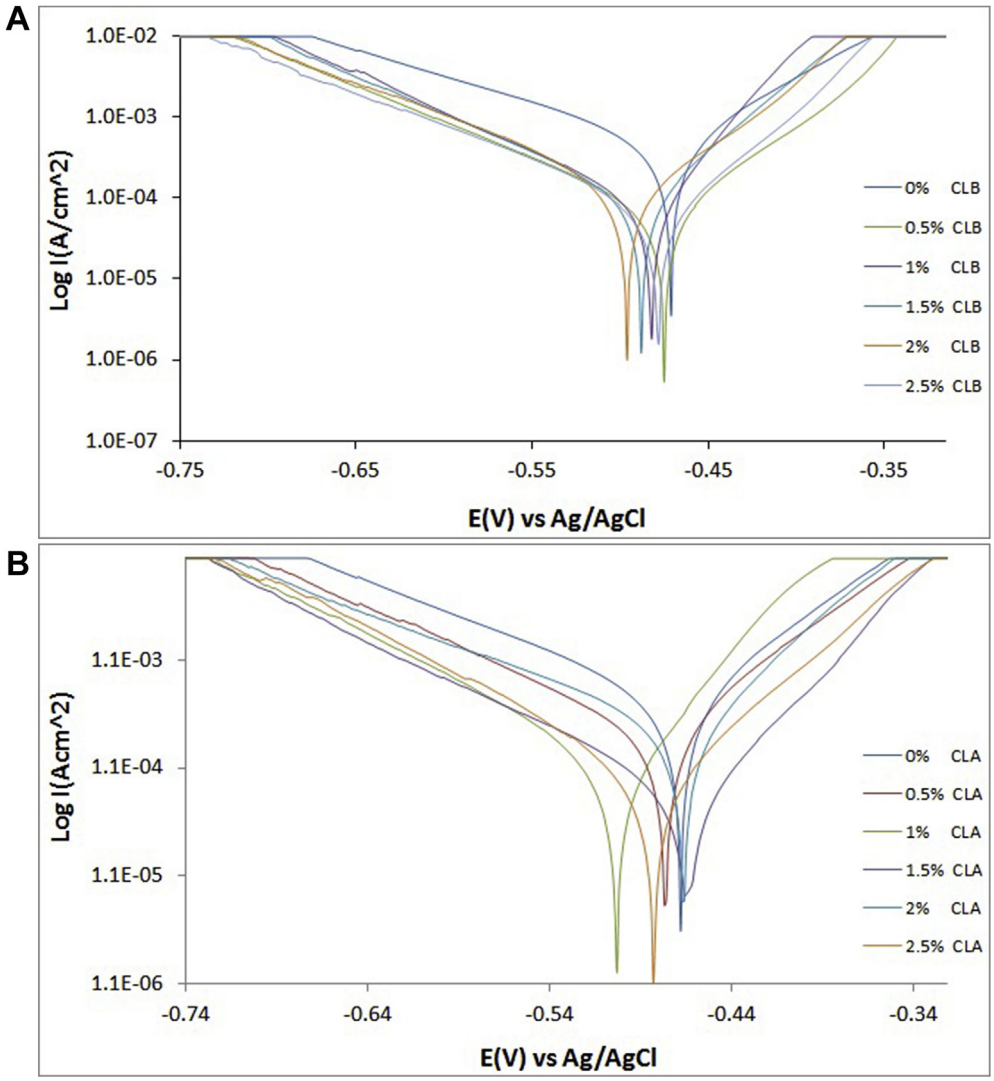


**Fig. 9.** Potentiodynamic polarization plots for LCS corrosion in HCl solution at 0% - 2.5% inhibitor concentration (a) CLB inhibitor and (b) CLA inhibitor.

**Table 3**
Potentiodynamic polarization data for LCS corrosion in $H_2SO_4$ solution at 0%–2.5% CLB and CLA inhibitor concentration.

| H2SO4-CLB | | | | | | | | | |
|---|---|---|---|---|---|---|---|---|---|
| Sample | CLB Conc. (%) | LCS Corrosion Rate (mm/y) | CLB Inhibition Efficiency (%) | Corrosion Current (A) | Corrosion Current Density (A/cm$^2$) | Corrosion Potential (V) | Polarization Resistance, $R_p$ (Ω) | Cathodic Tafel Slope, $B_c$ (V/dec) | Anodic Tafel Slope, $B_a$ (V/dec) |
| A | 0 | 9.19 | 0 | 8.95E-04 | 7.92E-04 | −0.432 | 9.46 | −7.243 | 7.900 |
| B | 0.5 | 6.20 | 32.52 | 6.04E-04 | 5.35E-04 | −0.438 | 178.40 | −8.115 | 10.210 |
| C | 1 | 1.45 | 84.23 | 1.41E-04 | 1.25E-04 | −0.466 | 184.40 | −8.355 | 19.160 |
| D | 1.5 | 1.29 | 85.97 | 1.26E-04 | 1.11E-04 | −0.486 | 192.15 | −8.434 | 21.830 |
| E | 2 | 1.56 | 83.02 | 1.52E-04 | 1.35E-04 | −0.467 | 178.17 | −6.362 | 16.656 |
| F | 2.5 | 1.18 | 87.16 | 1.15E-04 | 1.02E-04 | −0.448 | 223.70 | −7.043 | 24.620 |
| **H2SO4-CLA** | | | | | | | | | |
| **Sample** | **CLA Conc. (%)** | **LCS Corrosion Rate (mm/y)** | **CLA Inhibition Efficiency (%)** | **Corrosion Current (A)** | **Corrosion Current Density (A/cm$^2$)** | **Corrosion Potential (V)** | **Polarization Resistance, $R_p$ (Ω)** | **Cathodic Tafel Slope, $B_c$ (V/dec)** | **Anodic Tafel Slope, $B_a$ (V/dec)** |
| A | 0 | 9.19 | 0 | 8.95E-04 | 7.92E-04 | −0.432 | 9.46 | −7.243 | 7.900 |
| B | 0.5 | 3.71 | 59.61 | 3.62E-04 | 3.20E-04 | −0.463 | 71.08 | −6.778 | 11.840 |
| C | 1 | 1.45 | 84.23 | 1.41E-04 | 1.25E-04 | −0.456 | 246.30 | −5.022 | 16.412 |
| D | 1.5 | 0.73 | 92.10 | 7.07E-05 | 6.26E-05 | −0.433 | 363.40 | −5.245 | 20.550 |
| E | 2 | 0.76 | 91.73 | 7.40E-05 | 6.55E-05 | −0.462 | 348.64 | −6.252 | 19.500 |
| F | 2.5 | 1.09 | 88.13 | 1.06E-04 | 9.40E-05 | −0.461 | 287.90 | −8.702 | 20.020 |

**Table 4**
Potentiodynamic polarization data for LCS corrosion in HCl solution at 0%–2.5% CLB and CLA inhibitor concentration.

| HCl-CLB | | | | | | | | | |
|---|---|---|---|---|---|---|---|---|---|
| Sample | CLB Conc. (%) | LCS Corrosion Rate (mm/y) | CLB Inhibition Efficiency (%) | Corrosion Current (A) | Corrosion Current Density (A/cm$^2$) | Corrosion Potential (V) | Polarization Resistance, $R_p$ (Ω) | Cathodic Tafel Slope, $B_c$ (V/dec) | Anodic Tafel Slope, $B_a$ (V/dec) |
| A | 0 | 5.94 | 0 | 5.78E-04 | 5.12E-04 | −0.471 | 44.43 | −6.883 | 12.000 |
| B | 0.5 | 1.05 | 82.30 | 1.02E-04 | 9.06E-05 | −0.475 | 250.90 | −8.990 | 14.500 |
| C | 1 | 1.09 | 81.63 | 1.06E-04 | 9.41E-05 | −0.482 | 264.40 | −9.469 | 21.850 |
| D | 1.5 | 1.09 | 81.67 | 1.06E-04 | 9.38E-05 | −0.488 | 260.20 | −9.381 | 17.910 |
| E | 2 | 1.08 | 81.78 | 1.05E-04 | 9.33E-05 | −0.496 | 257.30 | −8.474 | 16.300 |
| F | 2.5 | 1.05 | 82.32 | 1.02E-04 | 9.05E-05 | −0.478 | 251.10 | −8.892 | 18.720 |
| **HCl-CLA Sample** | **CLA Conc. (%)** | **LCS Corrosion Rate (mm/y)** | **CLA Inhibition Efficiency (%)** | **Corrosion Current (A)** | **Corrosion Current Density (A/cm$^2$)** | **Corrosion Potential (V)** | **Polarization Resistance, $R_p$ (Ω)** | **Cathodic Tafel Slope, $B_c$ (V/dec)** | **Anodic Tafel Slope, $B_a$ (V/dec)** |
| A | 0 | 5.94 | 0 | 5.78E-04 | 5.12E-04 | −0.471 | 44.43 | −6.883 | 12.000 |
| B | 0.5 | 3.31 | 44.34 | 3.22E-04 | 2.85E-04 | −0.480 | 79.79 | −7.940 | 11.980 |
| C | 1 | 1.61 | 72.95 | 1.57E-04 | 1.38E-04 | −0.506 | 164.10 | −9.254 | 19.310 |
| D | 1.5 | 0.96 | 83.79 | 9.38E-05 | 8.30E-05 | −0.467 | 273.90 | −7.850 | 17.910 |
| E | 2 | 1.13 | 80.98 | 1.10E-04 | 9.74E-05 | −0.470 | 225.58 | −6.354 | 15.070 |
| F | 2.5 | 1.16 | 80.56 | 1.13E-04 | 9.96E-05 | −0.486 | 228.50 | −10.080 | 13.540 |

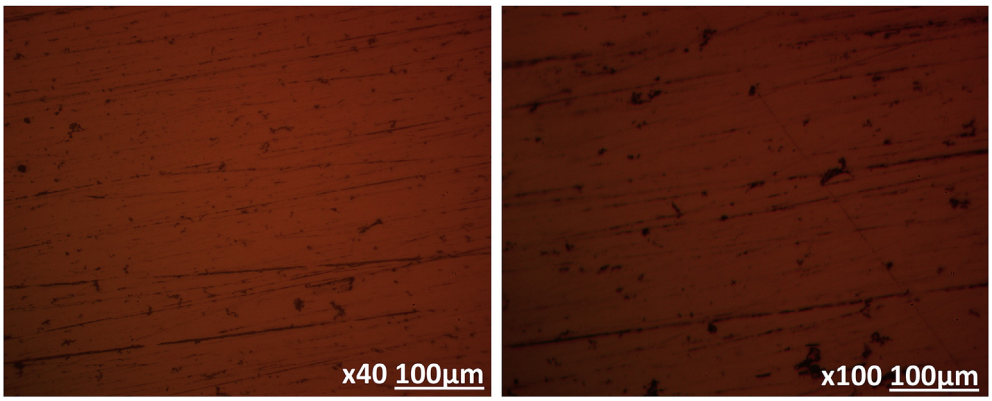


**Fig. 10.** Optical image of LCS before corrosion test.

not result in any significant change in value. This shows the inhibition performance of CLB and CLA inhibitor is under activation control whereby modification of the corrosive medium plays significant role in hindering the diffusion of cl-anions to the steel surface. This is further confirmed from the cathodic shift in corrosion potential of LCS for both inhibitors. However, the higher anodic Tafel values show there is strong possibility for surface coverage of LCS in the acid solution which significantly decreased anodic dissolution activity (see Fig. 9).

### 3.4. Optical microscopy analysis

Optical images (mag. ×40 and x100) of LCS before corrosion, after corrosion in $H_2SO_4$ and HCl solution with inhibitor and after corrosion in both acids at 0.5% and 2.5% CLB and CLA concentrations are shown from Fig. 10 to Fig. 15(b). Fig. 10 shows the images of LCS before corrosion test. Fig. 11(a) and (b) shows the images of LCS after corrosion in $H_2SO_4$ and HCl solution without the inhibitors. Figs. 12(a) and 13(b) shows the images of LCS after corrosion in $H_2SO_4$ solution at 0.5% and 2.5% CLB and CLA concentrations while Figs. 14(a) and 15(b) shows the images of LCS after corrosion in HCl solution at 0.5% and 2.5% CLB and CLA concentrations respectively. The image of LCS after corrosion in $H_2SO_4$ and HCl solution without CLB and CLA inhibitor [Fig. 11(a) and (b)] are generally similar. Severe deterioration of the steel surfaces is clearly visible on both figures, however the pits and deep grooves on Fig. 11(b) is due to the electrochemical action of $Cl^-$ anions whose actions tends to be localized compared to Fig. 11(a) where the action $SO_4^{2-}$ anions generally deteriorates the entire steel surface. Fig. 12(a) and (b) shows the optical images of LCS after corrosion in $H_2SO_4$ at 0.5% CLB and CLA. The optical images show less severe deterioration compared to the control steel specimen. Secondly the extent and morphology of deterioration are similar and agrees the results from coupon analysis signifying poor surface protection and corrosion inhibition. Increase in CLB and CLA concentration to 2.5% changed the morphology of LCS as shown in Fig. 13(a) and (b). The presence of excess inhibitor molecules shielded the steel surface of the debilitating action of corrosive anions. CLA inhibitor appears to be more effective [Fig. 13(b) compared to CLB [Fig. 13(a). Minimal surface deterioration is present in Fig. 13(a), though the surface discolorations are superficial and do not necessarily connote surface degradation. Observation of Fig. 14(a) and (b) CLB at 0.5% concentration in HCl performs more effectively than CLA. Though both images show significant morphological deterioration, the extent of deterioration on Fig. 14(b) is more severe. Molecules of CLA were ineffective in preventing the formation of corrosion pits resulting from the localized oxidation reactions by $Cl^-$ anions. The corresponding image in Fig. 14(a) shows CLB at lower concentration counteraction the electrochemical action of $Cl^-$ at 0.5% concentration. Increase in concentration of CLB [Fig. 15(a)] and CLA [Fig. 15(b)] to 2.5% significantly improved the morphology of LCS corresponding to effective corrosion inhibition. It is clearly visible that CLB demonstrated

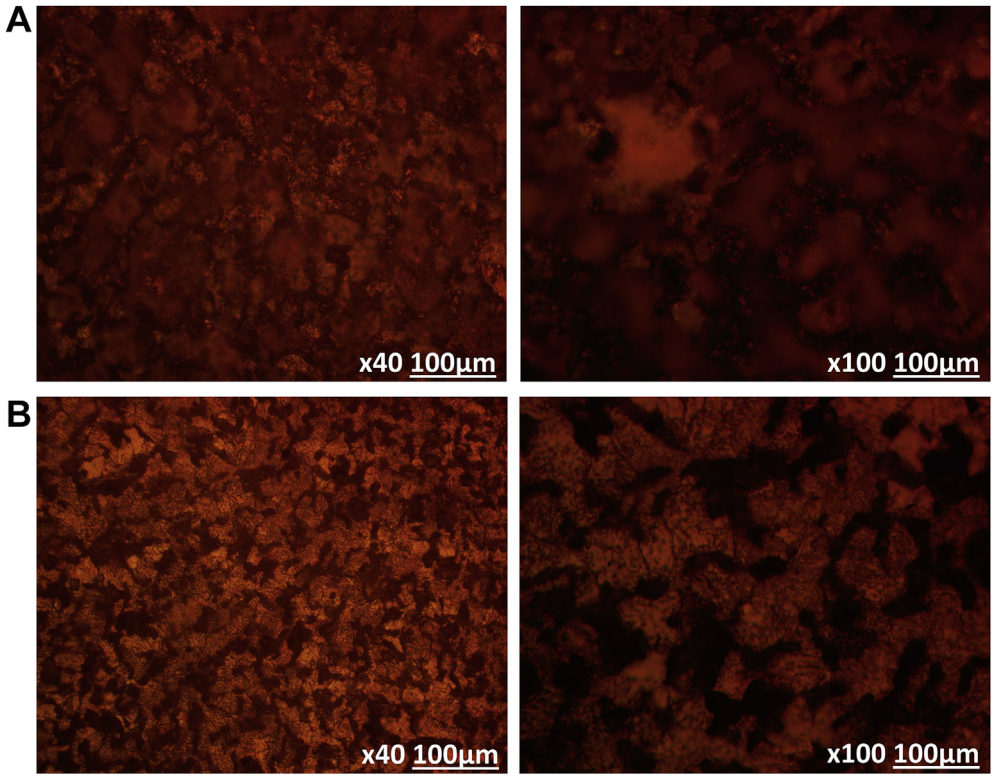


**Fig. 11.** Optical images of LCS after corrosion without inhibitor (a) from $H_2SO_4$ and (b) from HCl solution.

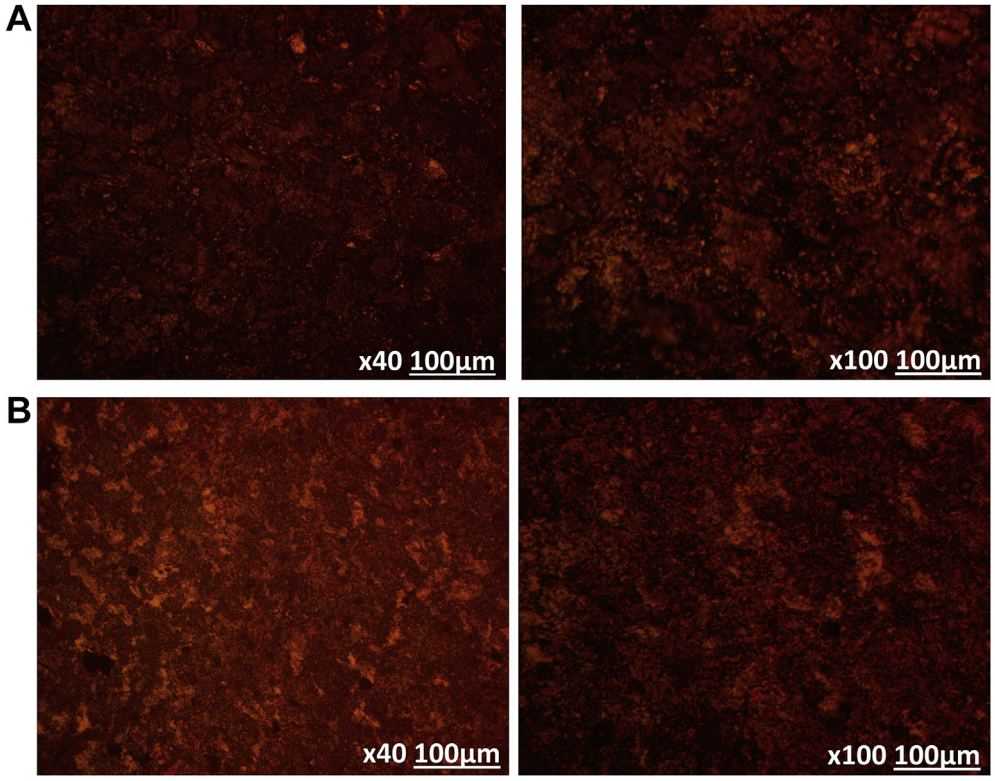


**Fig. 12.** Optical images LCS after corrosion in $H_2SO_4$ solution with inhibitor (a) CLB and (b) CLA at 0.5% concentration.

superficial vulnerability of general surface deterioration due to mild surface deterioration of LCS surface while CLA demonstrated slight weakness to localized corrosion as shown in the numerous micro deterioration on the surface which are somewhat superficial.

## 4. Conclusion

The combined admixture of clove essential oil extract with basil oil and atlas cedar oil effectively inhibited the corrosion of low carbon steel in dilute $H_2SO_4$ and HCl solution with corrosion inhibition

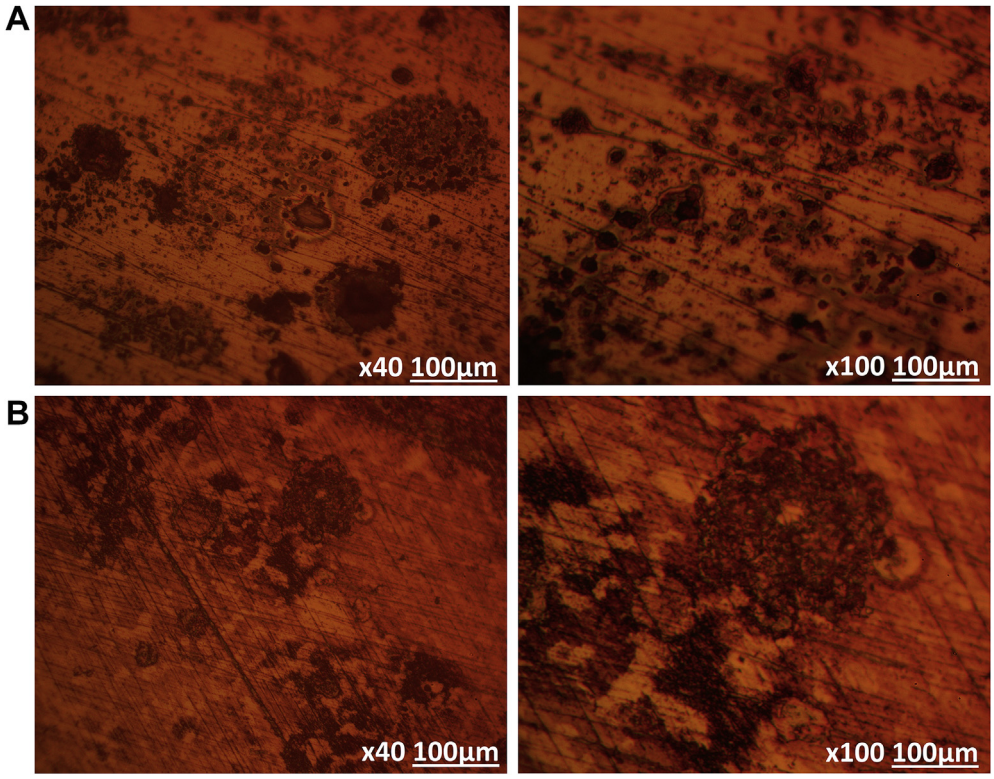


**Fig. 13.** Optical images LCS after corrosion in $H_2SO_4$ solution with inhibitor (a) CLB and (b) CLA at 2.5% concentration.

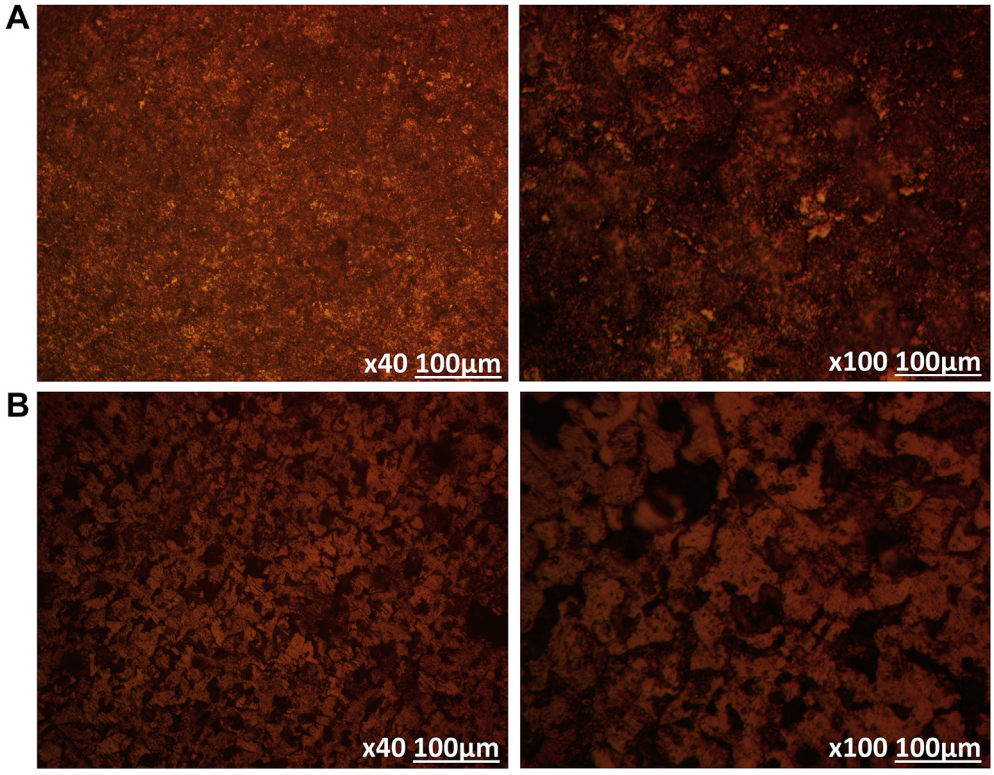


**Fig. 14.** Optical images LCS after corrosion in HCl solution with inhibitor (a) CLB and (b) CLA at 0.5% concentration.

efficiency generally above 80% at most inhibitor concentrations in both acids. The admixed inhibitor compounds demonstrated mixed inhibiting properties with dominant cathodic influence. Corrosion potential plots of the inhibited steel were significantly electropositive relative to the control in $H_2SO_4$ due to effective surface coverage and suppression of the electrochemical action of $SO_4^{2-}$ anions while in HCl, the plots were relatively electronegative due to their interaction with $Cl^-$ anions. Significant morphological improvement of the carbon steel in the presence of both inhibitors occurred in H2SO4 however, superficial deterioration of the steel which visibly contrast the corroded steel

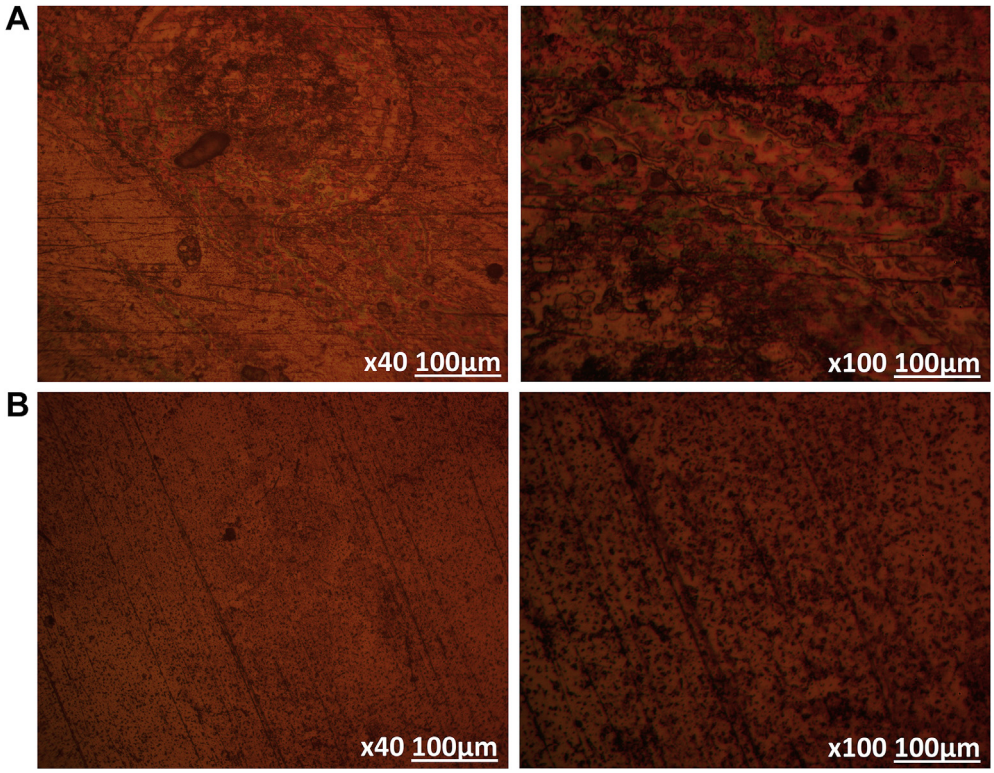


**Fig. 15.** Optical images LCS after corrosion in HCl solution with inhibitor (a) CLB and (b) CLA at 2.5% concentration.

without inhibitor occurred in HCl solution.

## Conflicts of interest

Authors declare no conflict of interest.

## Acknowledgements

The author acknowledges Covenant University Ota, Ogun State, Nigeria for the sponsorship and provision of research facilities for this project.

## References

Adardour, L., Saadouni, M., El Aoufir, Y., El khlifi, A., Kerroum, Y., Zarrouk, A., Guenbour, A., Taleb, M., Boukhriss, S., Oudda, H., 2018. Theoretical and experimental inhibitive properties of mild steel in phosphoric acid by clove essential oil. J. Mater. Environ. Sci. 9 (8), 2418–2430.

Afia, L., Benali, O., Salghi, R., Ebenso, E.E., Jodeh S, S., Zougagh, M., Hammouti, B., 2014. Steel corrosion inhibition by acid garlic essential oil as a green corrosion inhibitor and sorption behaviour. Int. J. Electrochem. Sci. 9, 8392–8406.

Ahmad, Z., 2006. Selection of Materials for Corrosive Environment, in Principles of Corrosion Engineering and Corrosion Control.

Bouoidina, A., Chaouch, M., Abdellaoui, A., Lahkimi, A., Hammouti, B., El-Hajjaji, F., Taleb, M., Nahle, A., 2017. Essential oil of "Foeniculum vulgare": antioxidant and corrosion inhibitor on mild steel immersed in hydrochloric medium. Anti-Corros. Method. M. 64 (5), 563–572. https://doi.org/10.1108/ACMM-10-2016-1716.

Dahmani, K., Galai, M., Cherkaoui, M., El hasnaoui, A., El Hessni, A., 2012. Cinnamon essential oil as a novel eco-friendly corrosion inhibitor of copper in 0.5 M sulfuric acid medium. J. Mater. Environ. Sci. 8 (9), 1676–1689.

El Ouadi, Y., Bouyanzer, A., Majidi, L., Paolini, J., Desjobert, J.M., Costa, J., Chetouani, A., Hammouti, B., 2014. Salvia officinalis essential oil and the extract as green corrosion inhibitor of mild steel in hydrochloric acid. J. Chem. Pharm. Res. 6 (7), 1401–1416.

El-Hajjaji, F., Abdellaoui, A., Taleb, M., Hammouti, B., Zarrouk, A., 2017. Chemical composition, anticorrosion and antioxidant activity of clove (Syzygium aromaticum) oil. J. Nat. Prod. 10, 45–57.

Gardner, L., 2008. Aesthetics, economics and design of stainless steel structures. Adv. Steel Constr. 4 (2), 113–122.

Halambek, J., Žutinić, A., Berković, K., 2013. Ocimum basilicum L. oil as corrosion inhibitor for aluminium in hydrochloric acid solution. Int. J. Electrochem. Sci. 8, 11201–11214.

Hamdani, I., El Ouariachi, E., Mokhtari, O., Salhi, A., Chahboun, N., ElMahi, B.A., Bouyanzer, A., Zarrouk, A., Hammouti, B., Costa, J., 2015. Chemical constituents and corrosion inhibition of mild steel by the essential oil of Thymus algeriensis in 1.0 M hydrochloric acid solution. Der Pharma Chem. 7 (8), 252–264.

Hmamou, D.B., Salghi, R., Zarrouk, A., Zarrouk, H., Errami, M., Hammouti, B., Afia, L., Bazzi, L., Bazzi, L., 2013. Adsorption and corrosion inhibition of mild steel in hydrochloric acid solution by verbena essential oil. Res. Chem. Intermed. 39, 973–989. https://doi.org/10.1007/s11164-012-0609-7.

Idouhli, R., Oukhrib, A., Koumya, Y., Abouelfida, A., Benyaich, A., Ahmed Benharref, A., 2017. Inhibitory effect of Atlas cedar essential oil on the corrosion of steel in 1 m HCl. Corros. Rev. 36 (4), 373–384. https://doi.org/10.1515/corrrev-2017-0076.

Loto, C.A., Loto, R.T., Popoola, A.P.I., 2011. Electrode potential monitoring of effect of plants extracts addition on the electrochemical corrosion behaviour of mild steel reinforcement in concrete. Int. J. Elect. Sci. 6 (8), 3452–3465.

Loto, R.T., 2016. Electrochemical analysis of the corrosion inhibition properties of 4-hydroxy-3-methoxybenzaldehyde on low carbon steel in dilute acid media. Cog. Eng. 3 (1), 1242107.

Loto, R.T., Oluwatobilola Olowoyo, O., 2018. Corrosion inhibition properties of the combined admixture of essential oil extracts on mild steel in the presence of SO42− anions. S. Afr. J. Chem. 26, 35–41. https://doi.org/10.1016/j.sajce.2018.09.002.

Loto, R.T., 2018a. Electrochemical analysis of the corrosion inhibition effect of trypsin complex on the pitting corrosion of 420 martensitic stainless steel in 2M H2SO4 solution. PLoS One 13 (4), e0195870. https://doi.org/10.1371/journal.pone.0195870.

Loto, R.T., 2018b. Surface coverage and corrosion inhibition effect of Rosmarinus officinalis and zinc oxide on the electrochemical performance of low carbon steel in dilute acid solutions. Results in Physics 8, 172–179. https://doi.org/10.1016/j.rinp.2017.12.003.

Loto, R.T., Leramo, R., Oyebade, B., 2018. Synergistic combination effect of salvia officinalis and lavandula officinalis on the corrosion inhibition of low-carbon steel in the presence of $SO_4^{2-}$ and $Cl^-$ containing aqueous environment. J. Fail. Anal. Prev. 18, 1429–1438. https://doi.org/10.1007/s11668-018-0535-0.

Loto, R.T., Loto, C.A., 2019. Electrochemical and microstructural analysis of the corrosion inhibition characteristics of atlas cedar essential oil extracts on mild steel in dilute $H_2SO_4$ and $C_6H_8O_7$ electrolytes. J. Bio Tribo Corros. 5, 39. https://doi.org/10.1007/s40735-019-0236-6.

Loto, R.T., Loto, C.A., Olaitan, A., 2019. Evaluation of the synergistic combination effect of four chemical compounds on the corrosion inhibition of carbon steel in dilute acid solutions. Chemical Data Collections 20, 100210. https://doi.org/10.1016/j.cdc.2019.100210.

Loto, R.T., Oghenerukewe, E., 2016. Inhibition studies of rosmarinus officinalis on the pitting corrosion resistance 439LL ferritic stainless steel in dilute sulphuric acid 32. pp. 2813–2832. (5). https://doi.org/10.13005/ojc/320557.

Narayanasamy, P., Ramachanderen, T., Natesan, M., Murugavel, S.C, S.C., 2009. Corrosion inhibition of mild steel by essential oils in an HCl environment. Mater. performance 48 (9), 52–56.

Ocheri, C., Ajani, O.O., Daniel, A., Agbo, N., 2017. The steel industry: a stimulus to national development. J. Powder Metall. Min. 6 (1), 156. https://doi.org/10.4172/2168-9806.1000156.

Prajapati, N.I., Vashi, R.T., 2017. Ocimum sanctum (Tulsi) leaves extract as corrosion inhibitor for aluminium in hydrochloric acid medium. Int. J. Innov. Res. Sci. Eng. Technol. 6 (8), 16376–16386.

Rekkab, S., Zarrok, H., Salghi, R., Zarrouk, A., Bazzi, Lh, Hammouti, B., Kabouche, Z., Touzani, R., Zougagh, M., 2012. Green corrosion inhibitor from essential oil of eucalyptus globulus (myrtaceae) for c38 steel in sulfuric acid solution. J. Mater. Environ. Sci. 3 (4), 613–627.

Roy, P., Karfa, P., Adhikari, U., Sukul, D., 2014. Corrosion inhibition of mild steel in acidic medium by polyacrylamide grafted Guar gum with various grafting percentage: effect of intramolecular synergism. Corros. Sci. 88, 246–253.

Saranya, J., Sowmiya, M., Sounthari, P., Parameswari, K., Chitra, S., Senthilkumar, K., 2016. N-heterocycles as corrosion inhibitors for mild steel in acid medium. J. Mol. Liq. 216, 42–52. https://doi.org/10.1016/j.molliq.2015.12.096.

Thomas, N.,V., Kim, S.-K., 2013. Beneficial effects of marine algal compounds in cosmeceuticals. Mar. Drugs 11 (1), 146–164. https://doi.org/10.3390/md11010146.

Verma, C., Olasunkanmi, L.O., Ebenso, E.E., Quraishi, M., Obot, I., 2016. Adsorption behavior of glucosamine-based, pyrimidine-fused heterocycles as green corrosion inhibitors for mild steel: experimental and theoretical studies. J. Phys. Chem. C 120 (21), 11598–11611. https://doi.org/10.1021/acs.jpcc.6b04429.

Verma, C., Quraishi, M., Kluza, K., Makowska-Janusik, M., Olasunkanmi, L.O., Ebenso, E.E., 2017. Corrosion inhibition of mild steel in 1M HCl by D-glucose derivatives of dihydropyrido [2, 3-d: 6, 5-d0] dipyrimidine-2, 4, 6, 8 (1H, 3H, 5H, 7H)-tetraone. Sci. Rep. 7, 44432. https://doi.org/10.1038/srep44432.

Winnik, S., 2008. Design for the Prevention of Corrosion-Under-Insulation. In Corrosion under Insulation (CUI) Guidelines.

Zarras, P., Stenger-Smith, J.D., 2014. Corrosion Processes and Strategies for Prevention: an Introduction. In Handbook of Smart Coatings for Materials Protection.